

Grain Orientation Influence on Residual Stress Distribution of Ground Surface of Blade Roots Made of Inconel 713LC

ČAPEK Jiří^{1,a}, GANCARCZYK Kamil^{2,b}, PITRMUC Zdeněk^{3,c}, KOLAŘÍK Kamil^{1,d}, MÁLEK Jaroslav^{4,e}, BERÁNEK Libor^{3,f}, GANEV Nikolaj^{1,g} and TROJAN Karel^{1,h}

¹ Department of Solid State Engineering, Faculty of Nuclear Sciences and Physical Engineering, Czech Technical University in Prague, Trojanova 13, 120 00 Prague 2, Czech Republic

² Department of Materials Science, Rzeszow University of Technology, al. Powstańców Warszawy 12, 35-959 Rzeszów, Poland

³ Department of Machining, Process Planning and Metrology, Faculty of Mechanical Engineering, Czech Technical University in Prague, Technická 4, 166 07 Prague 6, Czech Republic

⁴ Department of Materials Engineering, Faculty of Mechanical Engineering, Czech Technical University in Prague, Karlovo náměstí 13, 121 35 Prague 2, Czech Republic

^ajiri.capek@fjfi.cvut.cz, ^bkamilgancarczyk@prz.edu.pl, ^czdenek.pitrmuc@fs.cvut.cz,

^dkamil.kolarik@fjfi.cvut.cz, ^ejardamalek@seznam.cz, ^flibor.beranek@fs.cvut.cz,

^gnikolaj.ganev@fjfi.cvut.cz, ^hkarel.trojan@fjfi.cvut.cz

Keywords: Inconel 713LC, coarse-grain, grain orientation, omega-scan method, residual stresses.

Abstract. The aim of this contribution was to find whether there exists a relation between grains orientation in coarse-grained bulk material and macroscopic residual stress distribution after surface grinding. It could enable to predict that several coarse-grains are parallel to the primary (total) grinding force. Therefore, even smaller force can cause the slip (plastic deformation) and thereby smaller compressive residual stresses are determined in the very thin deformed surface layer. This effect can lead to degradation of some utility properties. In the case of a dynamically loaded nickel-based superalloy, it could lead to decrease of both the service life and the creep resistance.

Introduction

Inconel is two-phase material. The microstructure contains the nickel matrix (γ phase) and Ni_3Al precipitates (γ' phase). Nickel has a face centred cubic lattice (fcc) with regular structure, which is close-packing structure of atoms, therefore, the primary slip system is $\langle 110 \rangle \{111\}$. The number of slip systems is 12, which is sufficient amount to plastic deformation and it is the reason of plasticity of austenite-type materials. Precipitates Ni_3Al have ordered regular structure (L1_2), i.e. the primary slip system is $\langle 110 \rangle \{111\}$ too¹. Because bonds A-B are stronger than A-A type, yield strength of Ni_3Al phase is much higher in comparison with nickel matrix [2,3]. Moreover, these phases have coherent boundaries with

¹ In comparison with γ phase, L1_2 materials have anomalous yield strength. This anomalous originates from creation of four partial dislocations, two superintrinsic stacking fault and one antiphase boundary [1].

nickel grains, i.e. the dislocation movement through γ' phase is almost stopped due to its structure [2]. Therefore, these materials are hard, and very high strength or temperature is necessary to use to their phase deformation [4,5]. Moreover, Inconel 713LC is a work-hardening and creep-resistant material. Above temperature 600–800 °C, the precipitates lose their coherency and the strengthening is decreasing.

According to articles [6,7], the other material properties are poor thermal diffusivity, high temperature strength, presence of hard carbide phases or production of tough chip. Therefore, nickel-based superalloys are often used in automotive and aerospace industry as rotor turbine blades [8]. However, very stringent requirements on surface integrity specifically, residual stresses (RS) and microstructure are required, especially on blade roots [9]. Because of susceptibility to mechanical reinforcement of ground surface, the compressive RS are created in the surface layer in the case of adequate cooling. Nevertheless, the areas with potential accumulation of unfavourable tensile RS of γ/γ' phases on a macroscale can be localized by X-ray diffraction (XRD) techniques. Since the precipitates (γ' phase) are too hard to be plastically deformed, the local strain is very heterogeneous on a microscale – in the matrix channels, i.e. γ phase [2].

The anisotropy of polycrystalline bulk material is generally more reduced in comparison with single crystal because of the distribution of crystal orientation. The coarse-grained surface layers affected by grinding are crumbled to a fine-grained structure. In the case of coarse-grained bulk material, there may be several grains whose slip directions are parallel to the total grinding force². Therefore, even smaller force could cause the plastic deformation and thereby smaller compressive RS of surface fine-grained layers are determined [12]. Decreasing of favourable compressive RS can lead to reduction of the service life of dynamic loaded blades. For microstructure visibility, the electro-chemical etching of plastically deformed surface layer has to be done. Subsequently, XRD omega-scan (Ω -scan) method [13] or electron backscatter diffraction method (EBSD) [14] can be used for determination of the orientation of coarse-grains of bulk material from Inconel.

Experiment

The tested samples (blades) were casted from Inconel 713LC which is a nickel based superalloy. The nominal chemical composition (in wt.%) was following: 12.0 Cr, 5.7 Al, 4.6 Mo, 2.0 Nb, 0.7 Ti, 0.2 Fe, 0.1 Zr, 0.08 Co, 0.05 C, 0.013 B and balance of Ni.

Surfaces of three turbine blade roots (sample 1–3) with dimension 52×15 mm² were face ground. For grinding conditions see Figs. 3a–5a. Three areas were analysed by X-ray diffraction for residual stress determination on the blade root, namely I, II, see Fig. 1.

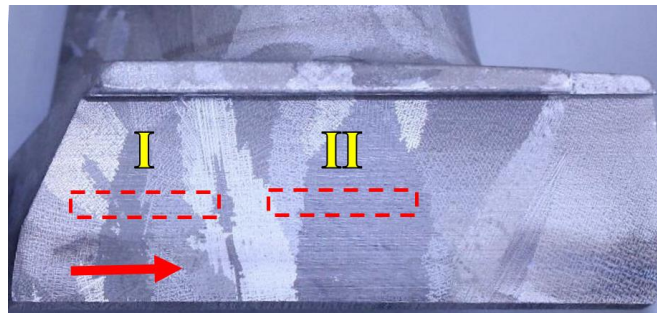


Figure 1: Experimental electro-chemical etched sample (blade root) with marked grinding direction and analysed areas I–II.

² Total grinding force is the sum of cutting, feed and passive forces whose magnitudes are given by grinding conditions, properties of grinding wheel and ground material: $\mathbf{F} = \sum_i \mathbf{F}_i$ [10,11].

PROTO iXRD COMBO diffractometer in ω -goniometer set-up was used to measure lattice deformations using manganese radiation. The diffraction lines $\{311\}$ of γ/γ' phases were analysed for obtaining macroscopic residual stresses [2]. *Rachinger's* method and *Absolute peak* method were used for determination of the diffraction angles $2\theta^{311}$ of the diffraction lines $K\alpha_1$. For the residual stress determination, $\sin^2\psi$ method with X-ray elastic constants $\frac{1}{2}s_2 = 6.57 \text{ TPa}^{-1}$, $s_1 = -1.56 \text{ TPa}^{-1}$ calculated from components of stiffness tensor ($C_{11} = 234.6 \text{ GPa}$; $C_{12} = 145.4 \text{ GPa}$; $C_{44} = 126.2 \text{ GPa}$) using Hill elastic model [15] were used. The cylinder collimator with diameter of 2 mm was inserted into the primary beam path. The blades were moving by $\pm 5 \text{ mm}$, therefore, the irradiated area was approx. $12 \times 2 \text{ mm}^2$, see Fig. 1. The average value of the effective penetration depth of $\text{MnK}\alpha$ radiation into the nickel-based material was approx. $4\text{--}5 \mu\text{m}$ [16].

The *ISO DEBYEFLEX 3003* equipment with chromium X-ray tube was used to back-reflection experiment for qualitative real structure determination. Using 30mm distance between radiation source and plate detector, the diffraction lines (Debye rings) $\{220\}$ of $K\alpha$ radiation and $\{311\}$ of $K\beta$ radiation of γ/γ' phases were obtained.

Evaluation of crystal orientation was based on measurements of α angle; i.e. the angle between crystallographic growth direction $\langle 100 \rangle$ and the main axis of the blade (perpendicular to grinding direction, see Fig. 1). The investigation was conducted with the use of X-ray diffraction method called omega-scan, utilizing prototype *OD-EFG* diffractometer invented and produced by *EFG* company (Berlin). The apparatus enables determination of the crystal orientation in the root and airfoil of turbine blade made of nickel-based superalloys. The size of the measuring spot was approx. 2 mm^2 and by this size; the orientation of whole surface of turbine blade can be mapped with an accuracy of $\pm 0.01^\circ$. Because of the method limitation, the unmeasurable α angles were set to zero.

The microstructure of specimens was studied with a *JEOL JSM 7600F* microscope equipped with *Nordly's EBSD* detector. The results were processed by *HKL Channel 5* software equipment.

Results and discussions

The microstructure of thin surface layers after grinding was fine-grained, see Fig. 2a. Analysing this surface, the inhomogeneous RS were determined on the ground surface, i.e. areas I–II, see Figs. 3a–5a. Therefore, the surfaces were electro-chemical etched for removing of surface layers affected by grinding (approx. 0.2 mm) to bulk material microstructure visibility, see Fig. 1, where the coarse-grained microstructure of bulk material was evident, see Fig. 2b.

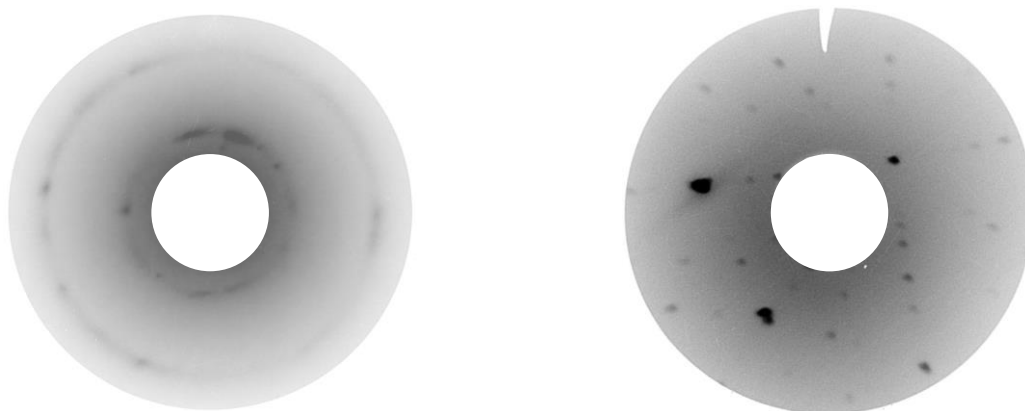


Figure 2a: The Debye rings of ground surface – fine grained structure. Figure 2b: The Debye rings of bulk material – coarse grained structure.

Although grinding usually leads to a creation of the tensile RS, the compressive RS were determined on the all surfaces of ground blades. Nevertheless, the tensile RS are predicted to the increasing of depth [11]. The compressive RS in the thin surface layers are caused by plastic deformation during grinding of the two-phase material which is prone to work-hardening. Moreover, the thermal conductivity of Inconel 713LC is approx. $4\times$ smaller in comparison with classic carbon steel which leads to insufficient heat distribution into chip and workpiece.

The etched samples were measured using the omega-scan method for gaining grain orientation of bulk material, see Figs. 3c–5c. The omega-scan method is relatively fast method in comparison with the EBSD, see Figs. 3b–5b. EBSD was selected as the comparative and verification method. It is necessary to note that X-ray radiation has an order of magnitude greater penetration depth than electrons. However, for this size of grains, it is not in this case important parameter.

Because of down grinding, i.e. the direction of the total grinding force points to the material, smaller force is necessary to use for deformation of grains with orientation in most cases between 20° and 70° in relation to surface, for facilitation around 45° . Using omega-scan method, deviation α angle was analysed. Because of three slip direction $\langle 110 \rangle$ of slip planes $\{111\}$, two possible values of α angle should be fit to gain. From relation of crystallography follows that 0° or 45° of α angle [17] is in relative to the orientation of total grinding force of 45° . Similarly, using EBSD method, two possible values of grain orientation are necessary to have, namely $\langle 100 \rangle$ or $\langle 111 \rangle$.

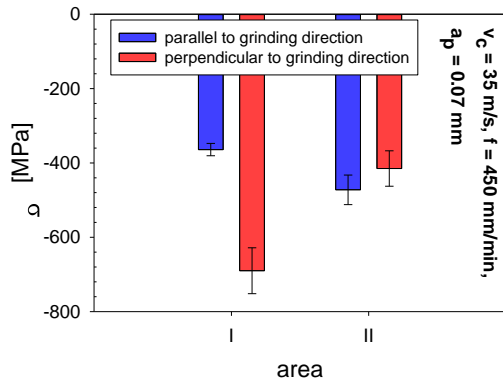


Figure 3a: RS of areas I–II on the surface of the sample 1.

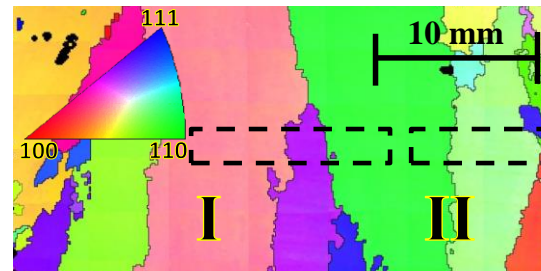


Figure 3b: EBSD orientation map of the sample 1.

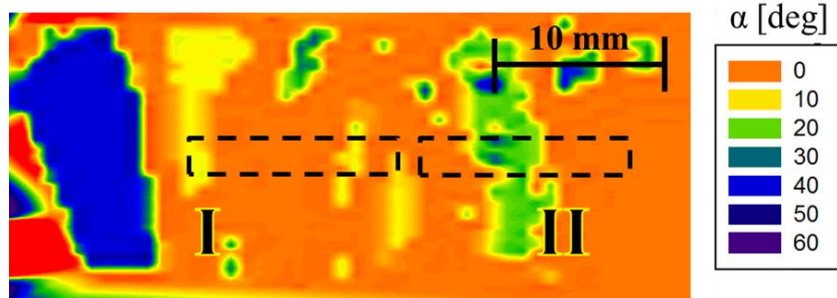


Figure 3c: Deviation angle α of omega-scan method of the sample 1.

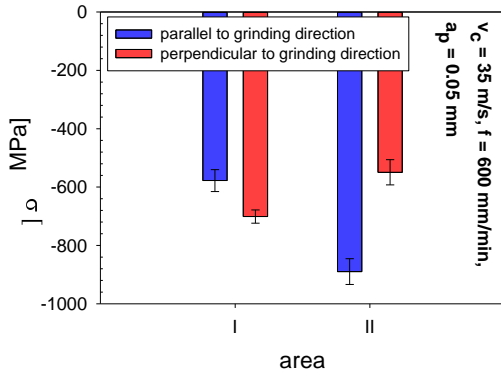


Figure 4a: RS of areas I–II on the surface of the sample 2.

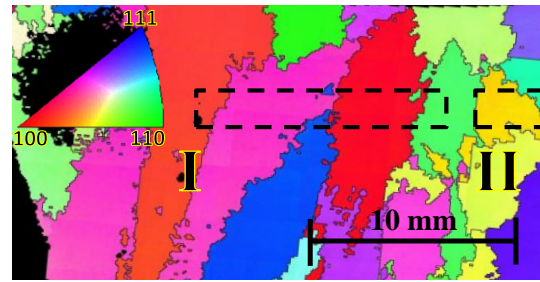


Figure 4b: EBSD orientation map of the sample 2.

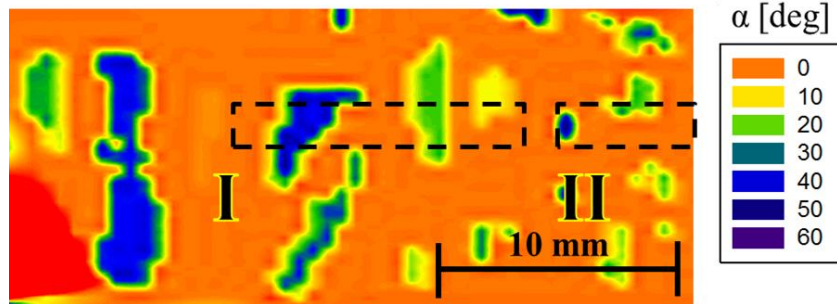


Figure 4c: Deviation angle α of omega-scan method of the sample 2.

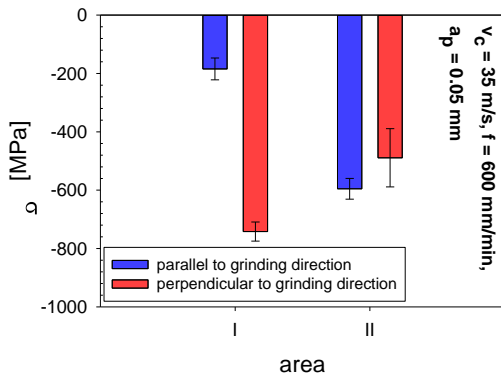


Figure 5a: RS of areas I–II on the surface of the sample 3.

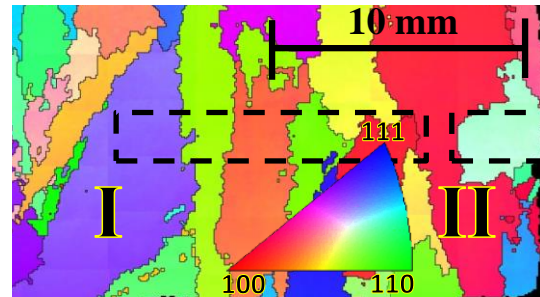


Figure 5b: EBSD orientation map of the sample 3.

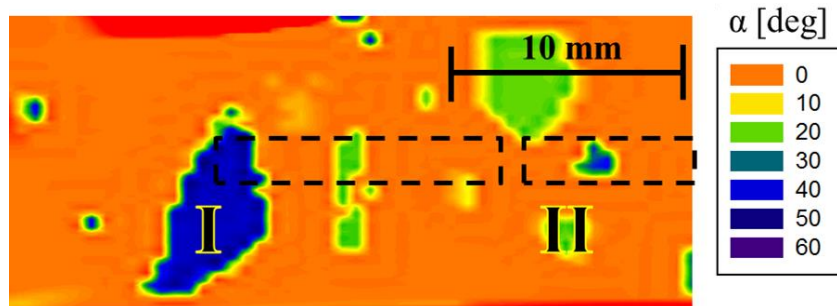


Figure 5c: Deviation angle α of omega-scan method of the sample 3.

In the case of areas I of sample 2 and 3, the compressive RS decreased in comparison with the area II in the grinding direction, see Figs. 4a and 5a. The decreasing should be caused by irradiated grains which have the deviations of α angle 40–50°, see Figs. 4c and 5c. The orientation of grains $\{111\}$ or $\{100\}$ is evident from EBSD, see Figs. 4b and 5b. These results are in accordance with expectation and before explained theory.

The RS are dependent on the grinding force in the direction perpendicular to grinding direction too. In general, the macroscopic RS on the ground surfaces should be compressive when cooled substantially during grinding and, moreover, the compressive RS in direction perpendicular to grinding are expected to be greater than in the grinding direction [9]. This statement could be not valid in the case of coarse-grained material. From Fig. 3c, it is evident that the orientation of irradiated grain of area II is approx. 20°. Therefore, the decreasing of the RS is significant too in the direction perpendicular to grinding direction, see Fig. 3a. The biggest decreasing of the RS values is for area II of sample. The influence on the total grinding force is not significant as in the case of α angle deviation 45°. From EBSD, the more general orientation of grains is evident, see Fig. 3b. On the other hand, incomplete area II was measured.

Conclusions

The present study showed:

- The thin ground surface layers determined by back-reflection X-ray diffraction show the fine-grained crystallographic real structure due to plastic deformation (the diffraction line is relatively continuous, and has homogeneous intensity around its perimeter, without any sign of texture). This is the reason why the surface RS of the samples can be determined by using X-ray diffraction.
- After removing of a surface layer 0.2 mm in thickness, the discrete diffraction spots were obtained which proves the considerable coarse-grained material comprised of single-crystal domains. This result is in correlation with metallographic pattern.
- The compressive RS of all ground surfaces with effective thickness approx. 4–5 μm were determined. In most cases, higher compressive RS were determined in the direction perpendicular to grinding direction. Due to mechanical interaction between cutting tool and material, the surface layers have tendency to elongate.
- The correlation between the decreasing of RS values of and orientation of the irradiated grains was established for both methods. Despite higher resolution and lower penetration depth of electrons, EBSD method with omega-scan method shows similar results.
- The limitation of α angle measurement is a disadvantage of this method. On the other hand, relatively fast measurements and easier preparation of samples are advantages of omega-scan method.

Acknowledgement

This work was supported by the governmental funding of Technological Agency of Czech Republic – project No. TA04010600 and the Grant Agency of the Czech Technical University in Prague, grant No. SGS16/245/OHK4/3T/14.

References

- [1] O.N. Mryasov, Y.N. Gornostyrev, M. Van Schilfgaarde, A.J. Freeman, Superdislocation core structure in $L1_2$ Ni_3Al , Ni_3Ge and Fe_3Ge : Peierls–Nabarro analysis starting from ab-initio, *Acta Mater.* 50 (2002) 4545-4554.
- [2] J. Li, R.P. Wahi, Investigation of γ/γ' lattice mismatch in the polycrystalline nickel-base superalloy IN738LC: Influence of heat treatment and creep deformation, *Acta Metall. Mater.* 43 (1995) 507-517.
- [3] P.C. Xia, J.J. Yu, X.F. Sun, H.R. Guan, Z.Q. Hu, Influence of γ' precipitate morphology on the creep property of a directionally solidified nickel-base superalloy, *Mater. Sci. Eng.: A.* 476.1 (2008) 39-45.
- [4] W. Österle, P.X. Li, Mechanical and thermal response of a nickel-base superalloy upon grinding with high removal rates, *Mater. Sci. Eng.: A.* 238.2 (1997) 357-366.
- [5] K. Kolařík, Z. Pala, L. Beránek, J. Čapek, Z. Vyskočil, N. Ganev, Non-Destructive Inspection of Surface Integrity in Milled Turbine Blades of Inconel 738LC, *Appl. Mech. Mater.* 486 (2014) 9-15.
- [6] E.O. Ezugwu, Z.M. Wang, A.R. Machado, The machinability of nickel-based alloys: a review, *J. Mater. Process. Tech.* 86.1–3 (1999) 1-16.
- [7] F. Tehovnik, J. Burja, B. Podgornik, M. Godec, F. Vode, Microstructural Evolution of Inconel 625 During Hot Rolling, *Mater. Tech.* 49.5 (2015) 801-806.
- [8] M. Petrenec, K. Obrtlík, J. Polák, T. Kruml, Fatigue behaviour of a cast nickel-based superalloy Inconel 792-5A at 700 °C, *Mater. Tech.* 40.5 (2006) 175-178.
- [9] J. Čapek, J. Kyncl, K. Kolařík, L. Beránek, Z. Pitrmuc, J. Medřický, Z. Pala, Grinding of Inconel 713 Superalloy for Gas Turbines, *Manuf. Technol.* 16.1 (2016) 38-45.
- [10] C. Xun, W.B. Rowe, Analysis and simulation of the grinding process. Part II: Mechanics of grinding, *Int. J. Mach. Tool. Manu.* 36.8 (1996) 883-896.
- [11] K. Vasilko, *Teória a prax trieskového obrábania*, COFIN, Prešov, 2009.
- [12] X. Zhang, T. Murakumo, Y. Koizumi, T. Kobayashi, H. Harada, Slip geometry of dislocations related to cutting of the γ' phase in a new generation single-crystal superalloy, *Acta Mater.* 51.17 (2003) 5073-5081.
- [13] K. Gancarczyk, R. Albrecht, C. Olesch, K. Kubiak, J. Sieniawski, Novel method for the measurement of crystalline perfection in single crystal turbine blades made of CMSX-4 superalloy, *Mater. Eng.* 208.6 (2015) 154-160.
- [14] T. Garcin, J.H. Schmitt, M. Militzer, In-situ laser ultrasonic grain size measurement in superalloy INCONEL 718, *J. Alloy. Compd.* 670 (2016) 329-336.
- [15] R. Hill, The elastic behaviour of a crystalline aggregate, *P. Phys. Soc.: A.* 65.5 (1952) 349.
- [16] J. Čapek, Z. Pala, Auxiliary programs for diffraction experiments, *Mater. Struct.* 22 (2015) 78-81.
- [17] I.L. Dillamore, Plasticity of Crystals with Special Reference to Metals, *Phys. Bull.* 20.3 (1969) 107.